Factors Determining the Asymmetry of ENSO

JIN LIANG AND XIU-QUN YANG

*China Meteorological Administration–Nanjing University Joint Laboratory for Climate Prediction
Studies, School of Atmospheric Sciences, and Jiangsu Collaborative Innovation Center of
Climate Change, Nanjing University, Nanjing, China*

DE-ZHENG SUN

Department of Atmospheric and Oceanic Sciences, University of Colorado, Boulder, Colorado

ABSTRACT

A fundamental aspect of the observed ENSO is the positive asymmetry between its two phases: the strongest El Niño is stronger than the strongest La Niña. The nonlinear term in the equation for the surface ocean heat budget has been theorized as a cause of the asymmetry. This theory is challenged by the diversity of asymmetry among the CMIP5 models: these models all employ primitive equations and thus have the nonlinear term in the heat budget equation for the ocean surface, yet the asymmetry simulated by these models ranges from significantly negative to significantly positive. Here, the authors employ an analytical but nonlinear model—a model that simulates the observed ENSO asymmetry—to show that the nonlinear heating term does not guarantee the oscillation in the system to possess positive asymmetry. Rather, the system can have regimes with negative, zero, and positive asymmetry. The regime in which the system finds itself depends on a multitude of physical parameters. Moreover, the range of certain physical parameters for the system to fall in the regime with positive asymmetry in the oscillation is rather narrow, underscoring the difficulty of simulating the observed ENSO asymmetry by CMIP5 models. Moreover, stronger positive asymmetry is found to be associated with a more complicated oscillation pattern: the two adjacent strongest warm events are spaced farther apart and more small events occur in between. These results deepen the understanding of factors that are behind the asymmetry of ENSO and offer paths to take to improve model-simulated ENSO asymmetry.

1. Introduction

ENSO, a natural "mode of oscillation" of the coupled tropical Pacific ocean–atmosphere system, affects climate and weather worldwide (Ropelewski and Halpert 1987; Huang and Wu 1989; Bove et al. 1998; Changnon 1999; McPhaden et al. 2006). While decades of intense studies of this phenomenon have advanced our understanding considerably (Neelin et al. 1998; Sun and Bryan 2010), there are aspects of it that still puzzle us. One example concerns its asymmetry, or the magnitude of the asymmetry between its two phases—the magnitude of El Niño on average tends to be bigger than the

magnitude of La Niña, and the strongest El Niño is stronger than the strongest La Niña (Burgers and Stephenson 1999; Kessler 2002; Hannachi et al. 2003).

This asymmetry is considered puzzling because it is not anticipated by prevailing dynamical theories of ENSO, either the delayed oscillatory theory (Battisti 1988; Suarez and Schopf 1988) or the more recent recharge oscillatory theory (Jin 1997; Meinen and McPhaden 2000). Nonlinear aspects of the ENSO system that have not been considered as essential are naturally considered as a cause. Using ocean assimilation data from NCEP (Carton et al. 2000), Jin et al. (2003) [see also An and Jin (2004) and Su et al. (2010)] calculated the nonlinear heating term in the surface heat budget equation for the eastern Pacific SST and found that the nonlinear dynamical heating (NDH) is positive for both the cold phase and the warm phase, thus offering an explanation for the asymmetry between the two phases. This explanation, however, is called into

---

ⓐ Denotes content that is immediately available upon publication as open access.

Corresponding author: Dr. Xiu-Qun Yang, xqyang@nju.edu.cn; Dr. De-Zheng Sun, dezheng.sun@colorado.edu
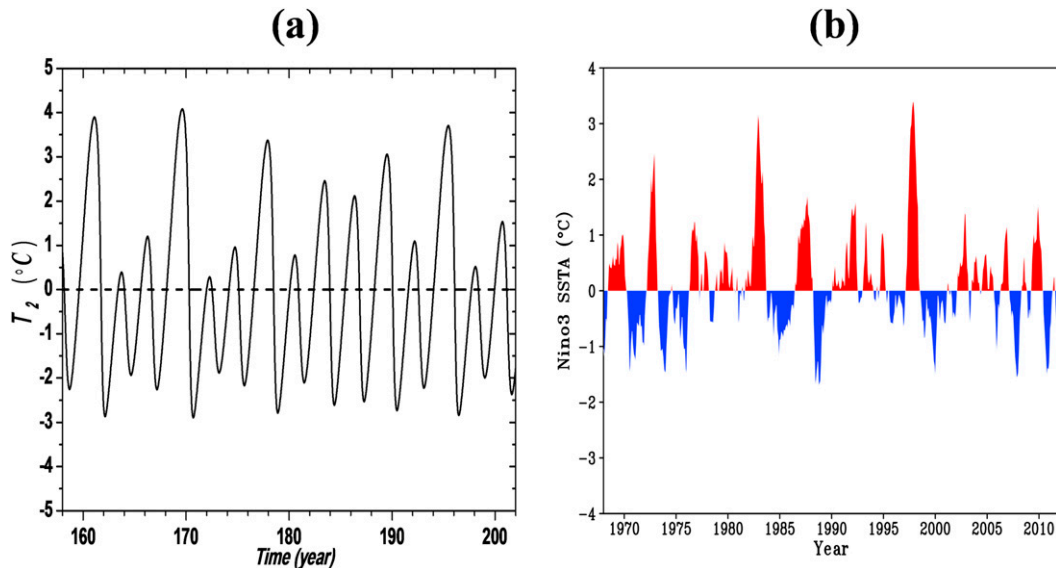
FIG. 1. Time series of the tropical eastern Pacific SST from the (a) nonlinear model of Sun (1997) and (b) real world. Note that both time series exhibit strong asymmetry between the warm and cold events. The parameters used for the time series from the model shown in (a) are the same as used for Fig. 5b in Liang et al. (2012) ($T_e = 31°C$, $s = 0.096$, $1/c = 150$ days, $1/r = 300$ days, and $\alpha/a = 3.0 \times 10^{-8}\,K^{-1}\,s^{-1}$). The time series for the real world are Niño-3 SST anomalies. The SST data for the real world are from the Hadley Centre for Climate Prediction and Research (Rayner et al. 1996).

question by the finding that the state-of-the-art CMIP5 models, which all have this nonlinear term in the heat budget equation for the tropical Pacific Ocean (Taylor et al. 2012), have serious problems in simulating ENSO asymmetry. In a limited set of CMIP5 models that have AMIP runs, Zhang and Sun (2014, see Fig. 1 therein) noted that all of the models severely underestimate the ENSO asymmetry. Some models even have negative asymmetry while most underestimate the positive asymmetry as found in the observations. A more recent study that encompasses the entire CMIP5 archive of twentieth-century simulations revealed that the problem of underestimating ENSO asymmetry is prevalent in almost all models, despite the fact that many models have a variance of ENSO that is twice as large as the observed (Sun et al. 2016).

The deficiency in our state-of-the-art models in simulating this fundamental aspect of ENSO is the motivation for the present study. Here we take the position that the nonlinear term in the heat budget equation is still a viable mechanism to give rise to the asymmetry in ENSO, but only when the system is in the correct dynamic regime, which is defined by a multitude of physical parameters. To help establish this position, we employ a lowest-order model for the coupled tropical Pacific Ocean–atmosphere system that is known to simulate ENSO asymmetry under the proper choice of parameters (Liang et al. 2012). In fact, the pattern of the oscillation with strong ENSO asymmetry from that

model closely resembles the observed (Fig. 1). Although the model in the present case may be considered simple, that does not undercut its ability to simulate ENSO oscillation with the observed characteristics, and it allows experiments to be conducted to examine the dependence of ENSO asymmetry on a suite of physical parameters corresponding to different physical processes. Moreover, each physical parameter can be varied over a sufficient range to force the model to traverse different dynamic regimes of which the model is capable. We suspect that the diversity in the simulated ENSO asymmetry from the CMIP5 models suggests that the models encompass different dynamical regimes that are characterized by oscillations of different patterns and thus different asymmetries. Because CMIP5 models have biased ENSO asymmetry, the complementary nature of simpler models to the state-of-the-art models [or more generally, as advocated by Held (2005), a hierarchy of climate models] is again highlighted. We are particularly curious about the diversity of ENSO asymmetry simulated in GCMs, which ranges from negative to positive values close to the observed, and we address this curiosity by taking advantage of the agility of the simple model, which allows us to conduct a set of sensitivity experiments. The goal is to shed some light on the question of why GCMs that have nonlinearity in the heat budget equation produce such diversity in their simulations of ENSO asymmetry. We also hope that

investigating the dependence of ENSO asymmetry on a multitude of physical parameters will result in suggestions of specific paths to take to alleviate the biases in GCM simulations of ENSO asymmetry. We are also interested in understanding how the system achieves a greater positive asymmetry. Does it achieve a greater positive asymmetry primarily through an increase in the magnitude of the warm events relative to the magnitude of the cold events, or through something more complex?

The paper is organized as follows. In section 2, we briefly describe the model. In section 3, we present the sensitivity study of the ENSO asymmetry to changes in the different parameters representing different physical processes. A summary and discussion are provided in section 4.

2. The model

We use the model of Sun (1997, 2000). It extends the model of Sun and Liu (1996) by including the thermocline dynamics. It has two predictive equations for the SST of the tropical Pacific—the SST of the western Pacific T_1 (120°E–155°W) and the SST of the eastern Pacific T_2 (155°–70°W), as

$$\frac{dT_1}{dt} = c(T_e - T_1) + sq(T_2 - T_1) \quad \text{and} \quad (1)$$

$$\frac{dT_2}{dt} = c(T_e - T_2) + q(T_{\text{sub}} - T_2), \quad (2)$$

and one predictive equation for the depth of thermocline of the western Pacific as

$$\frac{1}{r}\frac{dh_1'}{dt} = -h_1' + \frac{H_1}{2H_2}H\frac{\alpha}{b^2}(T_1 - T_2). \quad (3)$$

The left-hand sides of Eqs. (1), (2), and (3) are the time derivatives of corresponding variables, where T_{sub} is the subsurface ocean temperature, h_1' is the western equatorial thermocline anomaly, and H_1 is the depth of the mixed layer. Note that $H_2 = H - H_1$, with H being the zonal mean depth of the upper ocean at rest. Also, $b = c_k/L_x$, where c_k is the speed of the first baroclinic Kelvin wave. The formulation for the predictive equation for the depth of the thermocline of the western Pacific warm pool follows that of Jin (1996). The value of q is given by

$$q = \frac{\alpha}{a}(T_1 - T_2), \quad (4)$$

where a defines the adjustment time scale of the ocean currents to surface winds. The full set of equations can be found in Sun (1997) or Liang et al. (2012), with the latter having a more complete description of the model parameters. The model has been used to study the

decadal variability in El Niño events (Timmermann and Jin 2002a) and more recently to delineate the time-mean effects of ENSO on its decadal background state (Liang et al. 2012). A full list of the model parameters is provided in the appendix A of Liang et al. (2012). The set of physical parameters we will vary in our sensitivity study here are 1) the radiative–convective equilibrium of the sea surface temperature T_e; 2) the thermal damping coefficient from the atmosphere c; 3) the dynamical coupling strength between the atmosphere and ocean α; 4) the dynamical adjustment time scale for the equatorial upper ocean $(1/r)$; and 5) the relative strength between the zonal advection and the total equatorial upwelling s.

The radiative–convective equilibrium of SST is a measure of the intensity of radiative heating. It represents the SST that the surface ocean would attain if there were no ocean dynamics. More discussion of this parameter can be found in Sun and Liu (1996). The thermal damping coefficient from the atmosphere measures how fast an SST anomaly is damped by atmospheric processes alone. So, it is a function of atmospheric feedbacks [see Eq. (4) in Sun (2003)]. In fact, $1/c$ defines the time scale on which an SST anomaly is damped. The dynamical coupling strength between the atmosphere and ocean measures the sensitivity of the zonal wind stress to changes in the zonal SST gradients. The dynamical adjustment time scale for the equatorial upper ocean measures how fast the equatorial upper ocean adjusts to a new equilibrium with a change in the surface winds (i.e., the memory of the equatorial upper ocean) (Jin 1996). The relative strength of zonal advection can be given as $s = UH_1/WL_x$, where W and U are the upwelling and zonal velocity, respectively, and L_x and H_1 are the half-width of the basin and the depth of the mixed layer, respectively (Liang et al. 2012). With proper choices of these parameters, the model simulates the asymmetry of observed ENSO as well as the details in the corresponding oscillatory patterns as seen in the observations (Fig. 1).

We will investigate how the ENSO asymmetry in this model varies with the aforementioned key physical parameters. In line with earlier practice, we will use skewness of ENSO variability in the tropical eastern Pacific SST anomalies as the measure of ENSO asymmetry (Burgers and Stephenson 1999; Sun and Zhang 2006; An 2009). We will present corresponding changes in the amplitude of ENSO as well. The amplitude of ENSO will be measured by the standard variations in T_2. We integrate the model for 60 000 time steps, which corresponds to about 245 years. Data from the second half of the integration (years 123–245) are employed for the analysis. Despite the expectation, Sun et al. (2016) only found a weak correlation between the amplitude of ENSO and the asymmetry of ENSO. We are curious
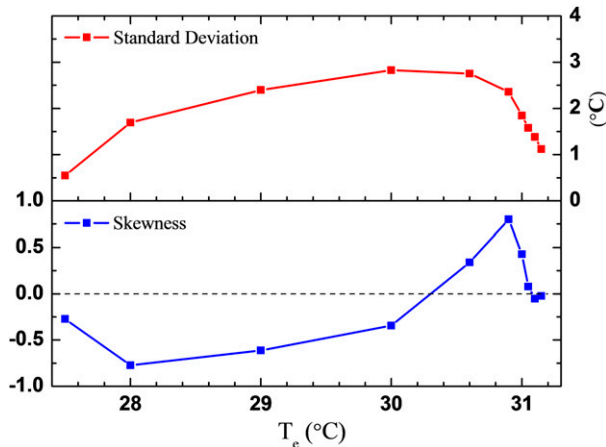
FIG. 2. (top) ENSO amplitude measured by the std dev of T_2 and (bottom) ENSO asymmetry measured by the skewness of variability in T_2 as a function of T_e.

about the relationship between the amplitude of ENSO and its asymmetry in this simple model as the different parameters are varied and more generally how the system achieves a greater asymmetry.

3. Results

a. Dependence of ENSO asymmetry on T_e

Figure 2 shows ENSO asymmetry as measured by the skewness of variability in T_2 (i.e., the SST of the tropical eastern Pacific) as a function of T_e. Also shown in the plot is ENSO amplitude (measured by the standard deviation of T_2). In Fig. 2, we see that as the value of T_e varies, ENSO asymmetry can be negative, zero, or positive. This confirms our suspicion that the non-linearity in the heat budget equation does not guarantee a positive ENSO asymmetry. In fact, as Fig. 2 shows, the regime with positive ENSO asymmetry corresponds to a rather narrow range of T_e, roughly from 30.3° to 31.0°C. In contrast, the regime with negative ENSO asymmetry corresponds to a much broader range of T_e. Over a broad range of T_e, the amplitude and asymmetry increase with increases in T_e. When T_e becomes very large (larger than ~30.6°C), the amplitude actually decreases with further increases in T_e. This is because the reference vertical temperature profile for the subsurface ocean is nonlinear [see Eq. (6) in Liang et al. (2012)] and thus the effective lapse rate of the thermocline—a key factor in determining the amplitude of ENSO—depends on the value of the depth of the thermocline [see Eq. (5) in Liang et al. (2012)], which in turn depends on the value of T_e [see Fig. 3 in Liang et al. (2012)]. Interestingly, the asymmetry does not decrease immediately as the amplitude starts to decrease,
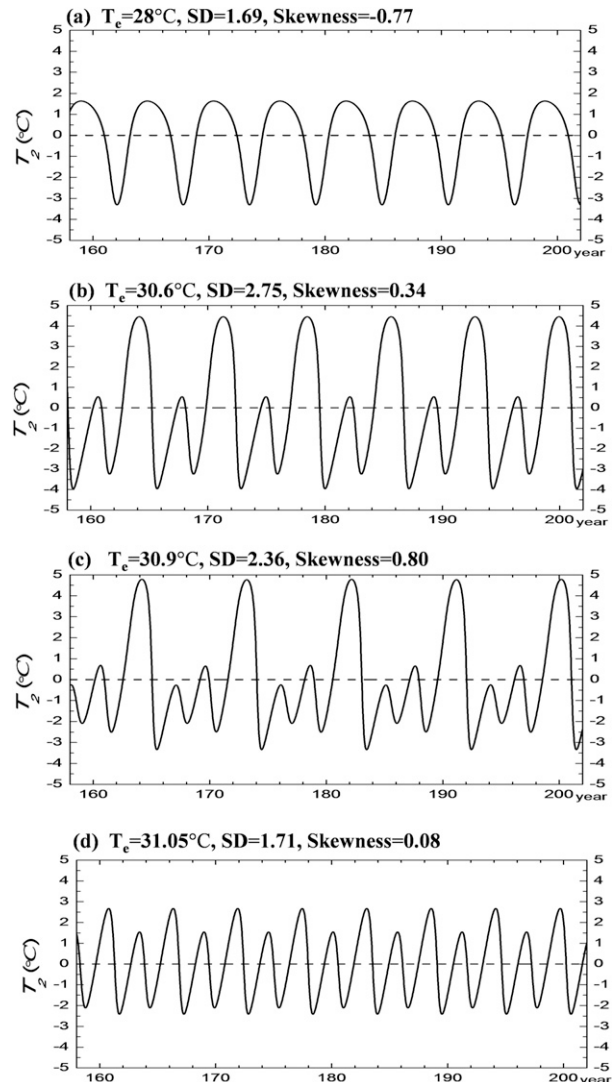

FIG. 3. Time series of T_2 under different values of T_e. The corresponding values of the std dev (°C) and skewness are indicated at the top of the time series. The skewness and std dev (SD) shown in the figure correspond to the periods shown but are the same when a much longer period is used.

providing an example that the two may not always go in the same direction. A similar situation is found in the figure when the amplitude is very small due to a weak value of T_e. The finding that whether amplitude and asymmetry go in the same direction depends on where the dynamic system is (i.e., the value of T_e) may serve as a theoretical footing to understand the finding by Sun et al. (2016) that, among CMIP5 simulations, the amplitude and asymmetry are only weakly positively correlated.

To understand in more detail how the system achieves a greater asymmetry as the value of T_e is varied, in Fig. 3 we show some actual time series of T_2 corresponding to different values of T_e. Figure 3a is a case
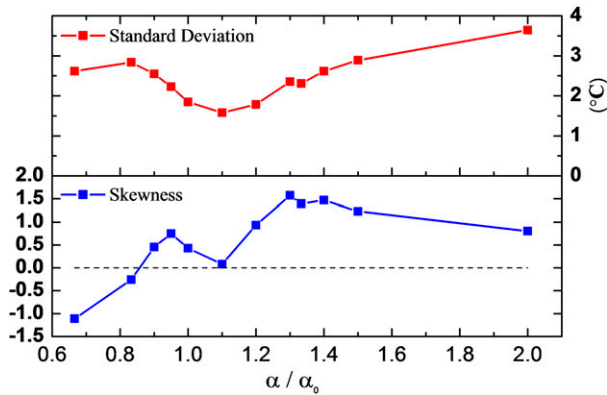
FIG. 4. (top) ENSO amplitude measured by the std dev of T_2 and (bottom) ENSO asymmetry measured by the skewness of variability in T_2 as a function of α/α_0, where α_0 is the parameter value used in Fig. 1a.

with a significantly negative asymmetry. Figures 3b and 3c give two cases with significantly positive asymmetry while the oscillation shown in Fig. 3d is nearly symmetric. Note that cases with positive asymmetry are characterized by a procession of strong warm events interrupted by smaller warm events, resembling the observed time series of tropical eastern Pacific SST (see Fig. 1, right). The symmetric case (Fig. 3d) shows that the magnitude of warm (cold) events does not have to be uniform to achieve symmetry. These time series show that a change in asymmetry tends to be associated with a change in the pattern of the oscillation, but not necessarily with a change in the mean amplitude. For example, the time series shown in Fig. 3d has a similar variance to that in Fig. 3a, but a much different asymmetry. The oscillation in Fig. 3c has a much greater positive asymmetry than that in Fig. 3b (0.80 vs 0.34), but the former actually has a smaller amplitude (2.36° vs 2.75°C). Overall, the four time series shown in the figure suggest a correspondence between an increase in skewness and an increase in the complexity in the pattern of oscillation. Oscillation in Fig. 3d is more complex than that in Fig. 3a in that the former has one additional event of a weaker magnitude in between the two adjacent strong events. In the oscillation shown in Fig. 3b, the magnitude of the weak warm event becomes even weaker relative to the strong one following it, compared with Fig. 3d. Oscillation in Fig. 3c has one more event between the two strongest events than the oscillation in Fig. 3b, and the former (Fig. 3c) has a greater positive skewness than the latter (Fig. 3b). The spacing between the two adjacent strongest events also increases as the skewness increases. It would be interesting to see whether time series of tropical eastern Pacific SST from those CMIP5 models that have a zero or near-zero asymmetry, a significantly negative asymmetry, and a significantly

positive asymmetry have the same characteristics as exhibited here in the time series shown in Fig. 3.

b. Dependence of ENSO asymmetry on α

As we have found with varying the value of T_e, varying α can also result in regimes with negative asymmetry, no asymmetry, or positive asymmetry (Fig. 4). This result reinforces the inference from Fig. 2 that whether the system has positive asymmetry really depends on where the system is, as defined by the value of α or T_e. Nonlinearity in the heat budget equation alone does not guarantee that the oscillation in the system will possess a significantly positive asymmetry.

Figure 4 also shows that with the exception of very large α, the asymmetry generally goes with the amplitude—large amplitude corresponds to a stronger (positive) asymmetry. But this positive correlation between the two breaks down when α becomes very large. Over the large range of the variation in the value of α in Fig. 4, the amplitude clearly does not always increase with the increase in α. This is again because the reference vertical temperature profile of the subsurface ocean is nonlinear [see Eq. (6) in Liang et al. (2012)] and consequently the effective lapse rate of the thermocline that is felt by the system [see Fig. 8 in Liang et al. (2012)] depends on where the system is.

The characteristics of the time series of T_2 corresponding to negative asymmetry, positive asymmetry, or near-zero asymmetry found by varying the values of α are very similar to those in the time series corresponding to these three regimes (as measured by the asymmetry) by varying the value of T_e (Fig. 5). Figure 5 shows a case with very strong asymmetry (skewness = 0.93) (Fig. 5d) and it is characterized by more weak warm events in between two very strong events relative to the case shown in Fig. 3c that also has strong asymmetry (skewness = 0.80), but not as strong as in Fig. 5d. Overall, it also confirms the inference we have from Fig. 3 that a change in the asymmetry is associated with a change in the oscillation pattern: the greater the asymmetry, the more complex the oscillation pattern. The change in the pattern associated with an increase in skewness is characterized by the appearance of one or more smaller events in between the original events and the spacing in between the strongest events increases.

c. Dependence of ENSO asymmetry on c

By varying the value of c, we again find that the system can have three regimes with negative asymmetry, zero asymmetry, and positive asymmetry, respectively (Fig. 6). However, it is interesting that at least over the range displayed, a range that encompasses a considerable variability in the amplitude of ENSO, asymmetry
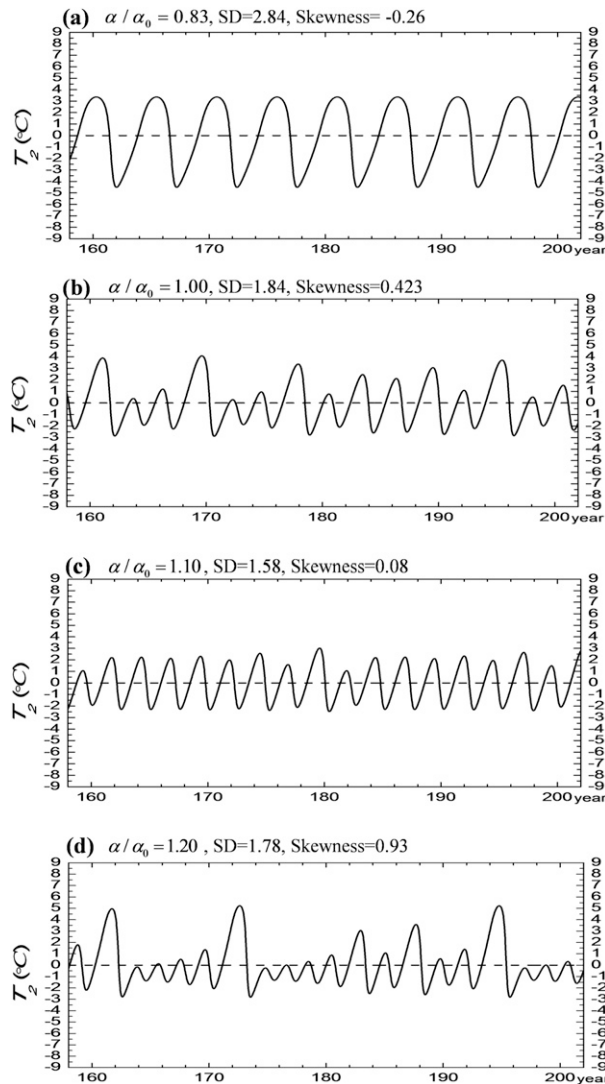
FIG. 5. Time series of T_2 under different values of α/α_0, where α_0 is the parameter value used in Fig. 1a. The corresponding values of the std dev (°C) and skewness are indicated at the top of the time series.
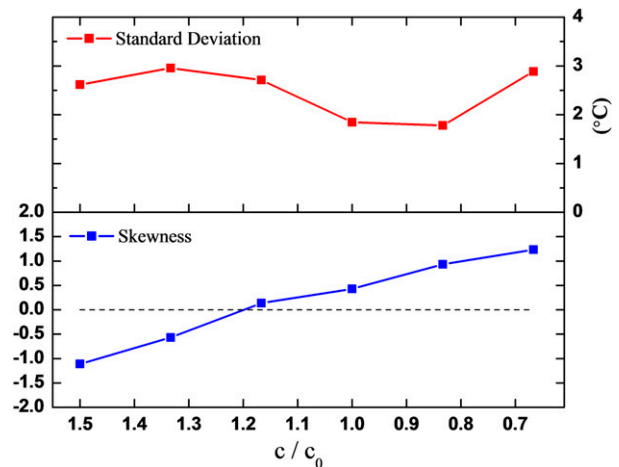

FIG. 6. (top) ENSO amplitude measured by the std dev of T_2 and (bottom) ENSO asymmetry measured by the skewness of variability in T_2 as a function of c/c_0, where c_0 is the reference value used in Fig. 1a. Note that c/c_0 is in decreasing order from the left to the right.

stronger skewness tends to correspond to a greater diversity in the magnitude of warm events and an increased spacing in time between the strongest warm events.

d. Dependence of ENSO asymmetry on s

We have also investigated the dependence of the asymmetry of ENSO on the strength of the zonal advection (relative to the total upwelling) as measured in the present model by the parameter s. The results are shown in Fig. 8. The corresponding amplitude of ENSO (as measured by standard deviation) is also plotted there in order to show its relationship with the asymmetry of ENSO. Again, we find that the oscillation in the system can have negative asymmetry, zero asymmetry, and positive asymmetry, depending on the value of s. The relationship between the amplitude and asymmetry is not linear over the range of the variations in the parameter s considered here. For small values of s ($s < 0.1$), the asymmetry stays positive and increases rapidly with the value of s. Timmermann et al. (2003) estimated that the value of s probably ranges from 0.04 to 0.1 in the present climate based on a GCM simulation. Figure 8 shows that this range of s corresponds to a regime with positive skewness as seen in the observations. For $s > 0.1$, the asymmetry starts to decrease rapidly to zero with the increase of s, and then becomes negative. In the regime with negative asymmetry, the asymmetry further decreases with increasing s, albeit at a much slower rate. Since most CGCMs have an excessive cold tongue (Sun et al. 2003; Sun et al. 2016), the value of s may likely be commonly overestimated in the CGCMs. The fact that larger s tends to result in weak or even negative

increases monotonically with a decreasing c: the less the damping from the atmosphere, the stronger the asymmetry. As shown by Jin et al. (2003), the nonlinear heating originating from the nonlinear term in the heat budget equation of the eastern Pacific Ocean surface [see the second term on the right-hand side of Eq. (2)] is the source for positive asymmetry, so the weaker the damping from the atmosphere (smaller c) is, the more time the system provides the asymmetry of ENSO to grow, leading to a stronger asymmetry.

Three time series of T_2 under different values of c are shown in Fig. 7. The corresponding asymmetry and magnitude measured by skewness and standard deviations are marked, respectively. These time series again show that a
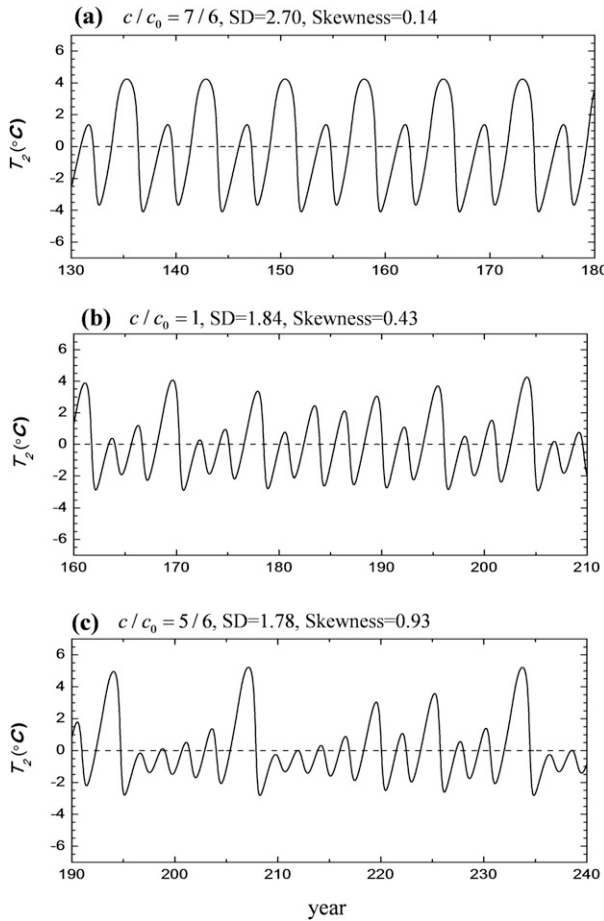
FIG. 7. Time series of T_2 under different values of c/c_0, where c_0 is the parameter value used in Fig. 1a. The corresponding values of the std dev (°C) and skewness are indicated at the top of the time series.

asymmetry as revealed here potentially links the excessive cold tongue to the weak or even negative asymmetry in many CGCMs.

e. Dependence of ENSO asymmetry on r

The weak or negative asymmetry can also be produced with a shorter memory of the equatorial upper ocean. Figure 9 shows a largely linear relationship between the ocean memory and the ENSO asymmetry. Note that the larger the parameter r, the shorter the corresponding ocean memory. Over a significant range of r ($r < 1.1$ times the standard value r_o; $r_o = 1/300$ days), the asymmetry is significantly positive. But as the value of r exceeds 1.1 times r_o, the asymmetry approaches zero and even becomes slightly negative. Note that $1/r$ corresponds to the time delay for the onset of the negative feedback in the delayed oscillatory theory (Battisti 1988; Suarez and Schopf 1988). The finding that the asymmetry increases with $1/r$ (i.e., decreases with increases in r)
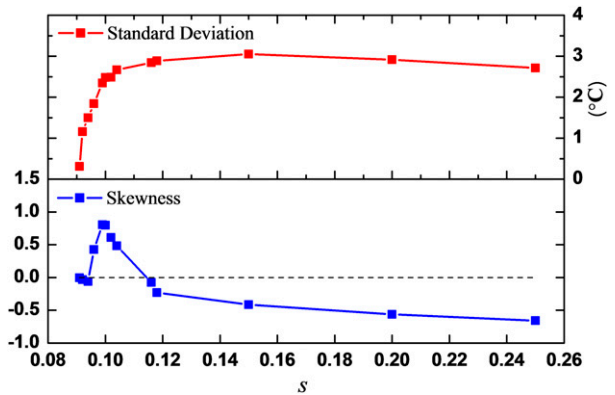

FIG. 8. Amplitude and asymmetry of ENSO measured by the std dev (°C) and skewness of the variability in T_2, respectively, as a function of the strength of the zonal advection parameter s.

may be explained by noting that a larger $1/r$ allows more time for the nonlinear heating to work on the growth of the asymmetry.

4. Summary and discussion

Motivated to better understand factors/parameters that may be involved in determining the ENSO asymmetry and to prepare a theoretical framework to shed light on the causes of the weak or even negative asymmetry shown in many state-of-the-art coupled GCMs, we resort to a simple model that has been shown to capture the observed major characteristics of ENSO including its asymmetry to investigate the role of a multitude of factors and/or parameters in determining the ENSO asymmetry. The methodology is to conduct sensitivity studies to quantify the dependence of the
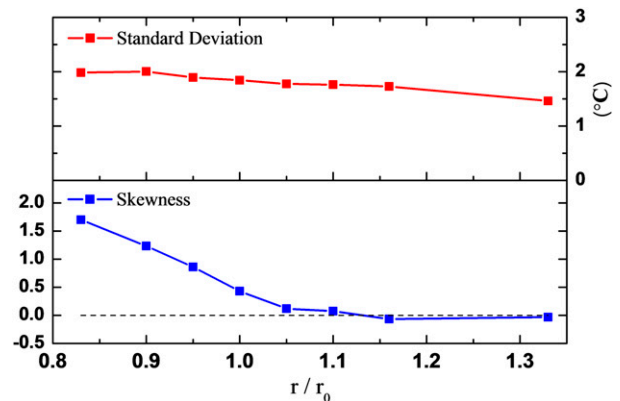

FIG. 9. Amplitude and asymmetry of ENSO measured by the std dev (°C) and skewness of the variability in T_2, respectively, as a function of the upper-ocean memory parameter r/r_0 (r_0 is the parameter value used in Fig. 1a). Note that increasing r corresponds to a shorter upper ocean memory.
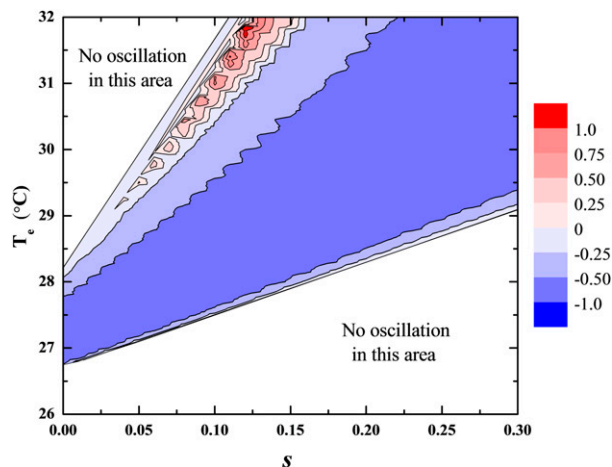
variability in the tropical eastern Pacific SST on these key physical parameters. The simplicity of the model allows such sensitivity studies to be conducted over a range of a chosen parameter that is not practical to be carried out with a fully coupled GCM.

The results from such a study show that different regimes corresponding to significantly positive, significantly negative, and zero or near-zero asymmetry are all found in the model. Which regime the coupled ENSO system finds itself in depends on the values chosen for the physical parameters. The dependence of the asymmetry on the thermal damping from the atmosphere and on the dynamical adjustment scale of the equatorial upper ocean is largely linear, but the relationship of the asymmetry with the radiative–convective equilibrium SST, the dynamical coupling strength, and the strength of the zonal advection relative to the upwelling is quite nonlinear. Only within a very narrow range for the radiative–convective equilibrium temperature and for the strength of the zonal advection is the system found to produce a positive ENSO asymmetry. This finding is further shown by recapping the dependence of the ENSO asymmetry as measured by the skewness of eastern Pacific SST on T_e and s using a more compact representation—a two-dimensional contour plot in Fig. 10. We observe in the figure that within the dynamic regime that has oscillation, the subregime for which the oscillation has a positive skewness occupies a rather narrow area. The figure thus provides an explanation for the apparent difficulty of the GCMs in simulating the observed positive ENSO asymmetry.

By varying these key physical parameters, we have also found that an increase in ENSO asymmetry is associated with a particular type of change in the oscillation patterns.

This change is characterized not by a uniform increase or decrease in the magnitudes of warm or cold events, but rather by an increase in the diversity of the magnitude of warm events. Such a change is also linked to a change in the time spacing between the strongest warm events (i.e., the extreme warm events). In particular, the significantly positive asymmetry is found to be associated with a more complicated oscillation pattern: the two adjacent strongest warm events are spaced farther apart and more small events occur in between. We would like to check these findings further in future work to see whether time series of tropical eastern Pacific SST from those CMIP5 models that have a zero or near-zero asymmetry, a significantly negative asymmetry, or a significantly positive asymmetry have the same characteristics or patterns as exhibited here in this simple model.

We are interested in applying some of the insights gained from the present theoretical model to more specifically diagnose sources of errors for ENSO asymmetry in some specific CMIP5 models. Note that both the radiative–convective equilibrium of the sea surface temperature (i.e., T_e) and the thermal damping coefficient from the atmosphere (i.e., c) are linked to the cloud feedbacks [see Eqs. (4) and (5) in Sun and Liu (1996)]; thus, the sensitivity of the ENSO asymmetry to T_e or c opens a path to look at the role of cloud feedbacks in simulating ENSO. Indeed, several studies have shown common biases in cloud feedbacks simulated by CMIP3 and CMIP5 models, the shortwave cloud feedback in particular (Sun et al. 2006, 2009; Bellenger et al. 2014; Li et al. 2015; Ying and Huang 2016). These studies have shown that the cloud shortwave feedback tends to be underestimated in the models, which will lead to a systematic error in the value of T_e or c, and thus is potentially a cause of the common bias in the ENSO asymmetry. We also note the recent study by Sun et al. (2016). They found significantly weak ENSO asymmetry and weakly nonlinear air–sea interaction over the tropical Pacific in CMIP5 climate models, compared with observation. Based on a statistical analysis, they suggested that a weak nonlinear air–sea interaction may play a role in the weak ENSO asymmetry. The present sensitivity results concerning the parameter α thus may provide a dynamic framework to understand findings from this statistical analysis by Sun et al. (2016).

Another interesting finding from this study that we are eager to exploit to better understand causes of outstanding biases in the climate models is the impact of a strong zonal advection (measured relative to the strength of the total equatorial upwelling) (i.e., s) on ENSO asymmetry. A very strong zonal advection can result in a very weak or even negative asymmetry. This finding potentially implicates the excessive cold tongue

that prevails in many CGCMs as a possible cause of the weak or even negative asymmetry of ENSO in these models (Li and Xie 2014; Li et al. 2016), as the excessive cold tongue likely implies an excessive zonal advection in these models. In addition, a weak ENSO asymmetry can also result from a shorter ocean memory (or a faster adjustment time for the equatorial upper ocean). As the upper-ocean adjustment time scale depends on the meridional scale of the winds (or SST) (Wang and An 2001; L. Chen et al. 2015), could the weak ENSO asymmetry in the state-of-the-art models suggest that the model ocean adjusts too quickly to wind change? This question clearly deserves further investigation.

Although in the present paper we have chosen to focus on the role of nonlinear heating term in the surface heat budget equation for the eastern Pacific SST in creating ENSO asymmetry, we realize that there are some other nonlinear processes that have been noted as potential candidates to explain ENSO asymmetry, such as the asymmetric negative feedback due to tropical oceanic instability waves (Vialard et al. 2001), which has a relatively stronger influence on the La Niña event, the nonlinear physics of the ocean mixed layer (Galanti et al. 2002), the nonlinear interaction between Madden–Julian oscillation and ENSO events (Kessler and Kleeman 2000), the biological–physical feedback process (Timmermann and Jin 2002b), and the nonlinear responses of the tropical atmospheric convection to El Niño and La Niña conditions (Hoerling et al. 1997; Kang and Kug 2002). We are also aware of other mechanisms that put more emphasis on the role of weather events. Levine et al. (2016) have suggested that the state dependence of weather events may play a role in giving rise to ENSO asymmetry. D. Chen et al. (2015) have suggested that the asymmetry, irregularity, and extremes of El Niño result from westerly wind bursts, a type of state-dependent atmospheric perturbation in the equatorial Pacific, since westerly wind bursts strongly affect El Niño but not La Niña because of their unidirectional nature. Monahan and Dai (2004) have pointed out that the anomalous wind field in the tropical western Pacific is dominated by westerly bursts that send downwelling Kelvin waves to the east and warm the SST there, thus on average making El Niño stronger than La Niña. These mechanisms, however, remain more qualitative than the mechanism of nonlinear dynamical heating on which the present paper focuses. Future studies will need to investigate more quantitatively to what degree these mechanisms may be responsible for the observed ENSO asymmetry and whether they can account for what we see in GCM simulations of this fundamental aspect of ENSO.

REFERENCES

An, S.-I., 2009: A review of interdecadal changes in the nonlinearity of the El Niño–Southern Oscillation. *Theor. Appl. Climatol.*, **97**, 29–40, doi:10.1007/s00704-008-0071-z.

——, and F.-F. Jin, 2004: Nonlinearity and asymmetry of ENSO. *J. Climate*, **17**, 2399–2412, doi:10.1175/1520-0442(2004)017<2399:NAAOE>2.0.CO;2.

Battisti, D. S., 1988: Dynamics and thermodynamics of a warming event in a coupled tropical atmosphere–ocean model. *J. Atmos. Sci.*, **45**, 2889–2919, doi:10.1175/1520-0469(1988)045<2889:DATOAW>2.0.CO;2.

Bellenger, H., É. Guilyardi, J. Leloup, M. Lengaigne, and J. Vialard, 2014: ENSO representation in climate models: From CMIP3 to CMIP5. *Climate Dyn.*, **42**, 1999–2018, doi:10.1007/s00382-013-1783-z.

Bove, M. C., J. J. O'Brien, J. B. Eisner, C. W. Landsea, and X. Niu, 1998: Effect of El Niño on U.S. landfalling hurricanes, revisited. *Bull. Amer. Meteor. Soc.*, **79**, 2477–2482, doi:10.1175/1520-0477(1998)079<2477:EOENOO>2.0.CO;2.

Burgers, G., and D. B. Stephenson, 1999: The "normality" of El Niño. *Geophys. Res. Lett.*, **26**, 1027–1030, doi:10.1029/1999GL900161.

Carton, J., G. Chepurin, X. Cao, and B. Giese, 2000: A Simple Ocean Data Assimilation analysis of the global upper ocean 1950–95. Part I: Methodology. *J. Phys. Oceanogr.*, **30**, 294–309, doi:10.1175/1520-0485(2000)030<0294:ASODAA>2.0.CO;2.

Changnon, S. A., 1999: Impacts of 1997–98 El Niño generated weather in the United States. *Bull. Amer. Meteor. Soc.*, **80**, 1819–1827, doi:10.1175/1520-0477(1999)080<1819:IOENOG>2.0.CO;2.

Chen, D., T. Lian, C. Fu, M. A. Cane, Y. Tang, R. Murtugudde, X. Song, Q. Wu, and L. Zhou, 2015: Strong influence of westerly wind bursts on El Niño diversity. *Nat. Geosci.*, **8**, 339–345, doi:10.1038/ngeo2399.

Chen, L., T. Li, and Y. Yu, 2015: Causes of strengthening and weakening of ENSO amplitude under global warming in four CMIP5 models. *J. Climate*, **28**, 3250–3274, doi:10.1175/JCLI-D-14-00439.1.

Galanti, E., E. Tziperman, M. Harrison, A. Rosati, R. Giering, and Z. Sirkes, 2002: The equatorial thermocline outcropping—A seasonal control on the tropical Pacific Ocean–atmosphere instability strength. *J. Climate*, **15**, 2721–2739, doi:10.1175/1520-0442(2002)015<2721:TETOAS>2.0.CO;2.

Hannachi, A., D. Stephenson, and K. Sperber, 2003: Probability-based methods for quantifying nonlinearity in the ENSO. *Climate Dyn.*, **20**, 241–256, doi:10.1007/s00382-002-0263-7.

Held, I. M., 2005: The gap between simulation and understanding in climate modeling. *Bull. Amer. Meteor. Soc.*, **86**, 1609–1614, doi:10.1175/BAMS-86-11-1609.

Hoerling, M. P., A. Kumar, and M. Zhong, 1997: El Niño, La Niña, and the nonlinearity of their teleconnections. *J. Climate*, **10**, 1769–1786, doi:10.1175/1520-0442(1997)010<1769:ENOLNA>2.0.CO;2.

Huang, R., and Y. Wu, 1989: The influence of ENSO on the summer climate change in China and its mechanism. *Adv. Atmos. Sci.*, **6**, 21–32, doi:10.1007/BF02656915.

Jin, F.-F., 1996: Tropical ocean–atmosphere interaction, the Pacific cold tongue, and the El Niño–Southern Oscillation. *Science*, **274**, 76–78, doi:10.1126/science.274.5284.76.

——, 1997: An equatorial ocean recharge paradigm for ENSO. Part I: Conceptual model. *J. Atmos. Sci.*, **54**, 811–829, doi:10.1175/1520-0469(1997)054<0811:AEORPF>2.0.CO;2.

——, S.-I. An, A. Timmermann, and J. Zhao, 2003: Strong El Niño events and nonlinear dynamical heating. *Geophys. Res. Lett.*, **30**, 1120, doi:10.1029/2002GL016356.

Kang, I. S., and J. S. Kug, 2002: El Niño and La Niña sea surface temperature anomalies: Asymmetry characteristics associated with their wind stress anomalies. *J. Geophys. Res.*, **107**, 4372, doi:10.1029/2001JD000393.

Kessler, W. S., 2002: Is ENSO a cycle or a series of events? *Geophys. Res. Lett.*, **29**, 2125, doi:10.1029/2002GL015924.

——, and R. Kleeman, 2000: Rectification of the Madden–Julian oscillation into the ENSO cycle. *J. Climate*, **13**, 3560–3575, doi:10.1175/1520-0442(2000)013<3560:ROTMJO>2.0.CO;2.

Levine, A. F. Z., F.-F. Jin, and M. J. McPhaden, 2016: Extreme noise–extreme El Niño: How state-dependent noise forcing creates El Niño–La Niña asymmetry. *J. Climate*, **29**, 5483–5499, doi:10.1175/JCLI-D-16-0091.1.

Li, G., and S.-P. Xie, 2014: Tropical biases in CMIP5 multimodel ensemble: The excessive equatorial Pacific cold tongue and double ITCZ problems. *J. Climate*, **27**, 1765–1780, doi:10.1175/JCLI-D-13-00337.1.

——, ——, Y. Du, and Y. Luo, 2016: Effects of excessive equatorial cold tongue bias on the projections of tropical Pacific climate change. Part I: The warming pattern in CMIP5 multi-model ensemble. *Climate Dyn.*, **47**, 3817–3831, doi:10.1007/s00382-016-3043-5.

Li, L. J., B. Wang, and G. J. Zhang, 2015: The role of moist processes in shortwave radiative feedback during ENSO in the CMIP5 models. *J. Climate*, **28**, 9892–9908, doi:10.1175/JCLI-D-15-0276.1.

Liang, J., X.-Q. Yang, and D.-Z. Sun, 2012: The effect of ENSO events on the tropical Pacific mean climate: Insights from an analytical model. *J. Climate*, **25**, 7590–7606, doi:10.1175/JCLI-D-11-00490.1.

McPhaden, M. J., S. E. Zebiak, and M. H. Glantz, 2006: ENSO as an integrating concept in Earth science. *Science*, **314**, 1740–1745, doi:10.1126/science.1132588.

Meinen, C. S., and M. J. McPhaden, 2000: Observations of warm water volume changes in the equatorial Pacific and their relationship to El Niño and La Niña. *J. Climate*, **13**, 3551–3559, doi:10.1175/1520-0442(2000)013<3551:OOWWVC>2.0.CO;2.

Monahan, A. H., and A. G. Dai, 2004: The spatial and temporal structure of ENSO nonlinearity. *J. Climate*, **17**, 3026–3036, doi:10.1175/1520-0442(2004)017<3026:TSATSO>2.0.CO;2.

Neelin, J. D., D. S. Battisti, A. C. Hirst, F.-F. Jin, Y. Wakata, T. Yamagata, and S. Zebiak, 1998: ENSO theory. *J. Geophys. Res.*, **103**, 14 261–14 290, doi:10.1029/97JC03424.

Rayner, N. A., E. B. Horton, D. E. Parker, C. K. Folland, and R. B. Hackett, 1996: Version 2.2 of the global sea-ice and sea surface temperature data set, 1993–1994. Hadley Centre Climate Research Tech. Note 74 (CRTN74), 46 pp. [Available online at http://www.metoffice.gov.uk/hadobs/gisst/crtn74.pdf.]

Ropelewski, C. F., and M. S. Halpert, 1987: Global and regional scale precipitation patterns associated with the El Niño/Southern Oscillation. *Mon. Wea. Rev.*, **115**, 1606–1626, doi:10.1175/1520-0493(1987)115<1606:GARSPP>2.0.CO;2.

Su, J., R. Zhang, T. Li, X. Rong, J.-S. Kug, and C.-C. Hong, 2010: Causes of the El Niño and La Niña amplitude asymmetry in the equatorial eastern Pacific. *J. Climate*, **23**, 605–617, doi:10.1175/2009JCLI2894.1.

Suarez, M. J., and P. S. Schopf, 1988: A delayed action oscillator for ENSO. *J. Atmos. Sci.*, **45**, 3283–3287, doi:10.1175/1520-0469(1988)045<3283:ADAOFE>2.0.CO;2.

Sun, D.-Z., 1997: El Niño: A coupled response to radiative heating? *Geophys. Res. Lett.*, **24**, 2031–2034, doi:10.1029/97GL01960.

——, 2000: Global climate change and ENSO: A theoretical framework. *El Niño: Historical and Paleoclimatic Aspects of the Southern Oscillation, Multiscale Variability, and Global and Regional Impacts*, H. F. Diaz and V. Markgraf, Eds., Cambridge University Press, 443–463.

——, 2003: A possible effect of an increase in the warm-pool SST on the magnitude of El Niño warming. *J. Climate*, **16**, 185–205, doi:10.1175/1520-0442(2003)016<0185:APEOAI>2.0.CO;2.

——, and Z. Y. Liu, 1996: Dynamic ocean–atmosphere coupling: A thermostat for the tropics. *Science*, **272**, 1148–1150, doi:10.1126/science.272.5265.1148.

——, and T. Zhang, 2006: A regulatory effect of ENSO on the time-mean thermal stratification of the equatorial upper ocean. *Geophys. Res. Lett.*, **33**, L07710, doi:10.1029/2005GL025296.

——, and F. Bryan, Eds., 2010: *Climate Dynamics: Why Does Climate Vary? Geophys. Monogr.*, Vol. 189, Amer. Geophys. Union, 216 pp.

——, J. Fasullo, T. Zhang, and A. Roubicek, 2003: On the radiative and dynamical feedbacks over the equatorial Pacific cold tongue. *J. Climate*, **16**, 2425–2432, doi:10.1175/2786.1.

——, and Coauthors, 2006: Radiative and dynamical feedbacks over the equatorial cold tongue: Results from nine atmospheric GCMs. *J. Climate*, **19**, 4059–4074, doi:10.1175/JCLI3835.1.

——, Y. Yu, and T. Zhang, 2009: Tropical water vapor and cloud feedbacks in climate models: A further assessment using coupled simulations. *J. Climate*, **22**, 1287–1304, doi:10.1175/2008JCLI2267.1.

Sun, Y., F. Wang, and D.-Z. Sun, 2016: Weak ENSO asymmetry due to weak nonlinear air–sea interaction in CMIP5 climate models. *Adv. Atmos. Sci.*, **33**, 352–364, doi:10.1007/s00376-015-5018-6.

Taylor, K. E., R. J. Stouffer, and G. A. Meehl, 2012: An overview of CMIP5 and the experiment design. *Bull. Amer. Meteor. Soc.*, **93**, 485–498, doi:10.1175/BAMS-D-11-00094.1.

Timmermann, A., and F.-F. Jin, 2002a: A nonlinear mechanism for decadal El Niño amplitude changes. *Geophys. Res. Lett.*, **29**, 1003, doi:10.1029/2001GL013369.

——, and ——, 2002b: Phytoplankton influences on tropical climate. *Geophys. Res. Lett.*, **29**, 2104, doi:10.1029/2002GL015434.

——, ——, and J. Abshagen, 2003: A nonlinear theory for El Niño bursting. *J. Atmos. Sci.*, **60**, 152–165, doi:10.1175/1520-0469(2003)060<0152:ANTFEN>2.0.CO;2.

Vialard, J., C. Menkes, J.-P. Boulanger, P. Delecluse, E. Guilyardi, M. J. McPhaden, and G. Madec, 2001: A model study of oceanic mechanisms affecting equatorial Pacific sea surface temperature during the 1997–98 El Niño. *J. Phys. Oceanogr.*, **31**, 1649–1675, doi:10.1175/1520-0485(2001)031<1649:AMSOOM>2.0.CO;2.

Wang, B., and S.-I. An, 2001: Why the properties of El Niño changed during the late 1970s. *Geophys. Res. Lett.*, **28**, 3709–3712, doi:10.1029/2001GL012862.

Ying, J., and P. Huang, 2016: Cloud–radiation feedback as a leading source of uncertainty in the tropical Pacific SST warming pattern in CMIP5 models. *J. Climate*, **29**, 3867–3881, doi:10.1175/JCLI-D-15-0796.1.

Zhang, T., and D.-Z. Sun, 2014: ENSO asymmetry in CMIP5 models. *J. Climate*, **27**, 4070–4093, doi:10.1175/JCLI-D-13-00454.1.